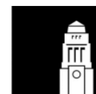

UNIVERSITY OF LEEDS

This is a repository copy of *A practical characterisation protocol for liquid-phase synthesised heterogeneous graphene*.

White Rose Research Online URL for this paper:
https://eprints.whiterose.ac.uk/161590/

Version: Supplemental Material

Article:

Lin, L-S, Bin-Tay, W, Li, Y-R et al. (3 more authors) (2020) A practical characterisation protocol for liquid-phase synthesised heterogeneous graphene. Carbon, 167. pp. 307-321. ISSN 0008-6223

https://doi.org/10.1016/j.carbon.2020.06.008

© 2020 Elsevier Ltd. All rights reserved. This manuscript version is made available under the CC-BY-NC-ND 4.0 license http://creativecommons.org/licenses/by-nc-nd/4.0/

Reuse

This article is distributed under the terms of the Creative Commons Attribution-NonCommercial-NoDerivs (CC BY-NC-ND) licence. This licence only allows you to download this work and share it with others as long as you credit the authors, but you can't change the article in any way or use it commercially. More information and the full terms of the licence here: https://creativecommons.org/licenses/

Takedown

If you consider content in White Rose Research Online to be in breach of UK law, please notify us by emailing eprints@whiterose.ac.uk including the URL of the record and the reason for the withdrawal request.

eprints@whiterose.ac.uk
https://eprints.whiterose.ac.uk/

Supplementary information

S1. The Raman 2D peak evolution

A baseline subtraction was carried out, followed by deconvolution of the 2D band into four vibrational elements using the Levenberg-Marquardt algorithm and the Lorentz peak model, in which the peak width of each elements (FWHM) were constrained to be ≤ 30 cm-1. These vibrational elements are: (1) $2D_{1B}$ with a peak centre at ~2660 cm^{-1}, corresponding to the P_{22} process; (2) and (3) $2D_{1A}$ and $2D_{2A}$ at ~2685 cm^{-1} and ~2710 cm^{-1} respectively, which correspond to the P_{12} and P_{21} processes and which have higher relative intensities in multilayer graphene; (4) $2D_{2B}$ at ~2730 cm^{-1} which is the highest frequency vibrational mode of the 2D band and is associated with the P_{11} process. This resulted in a fit with an adjusted R-Squared value ≥ 0.97.

Figure S1 (a) shows the Raman 2D peak of monolayer graphene, bilayer graphene and graphite from the previous work of Ferrari [1]. Monolayer graphene exhibits only a single Lorentzian peak at ~2685 cm^{-1}($2D_{1B}$), while for bilayer graphene (N ≥ 2), three additional peaks become

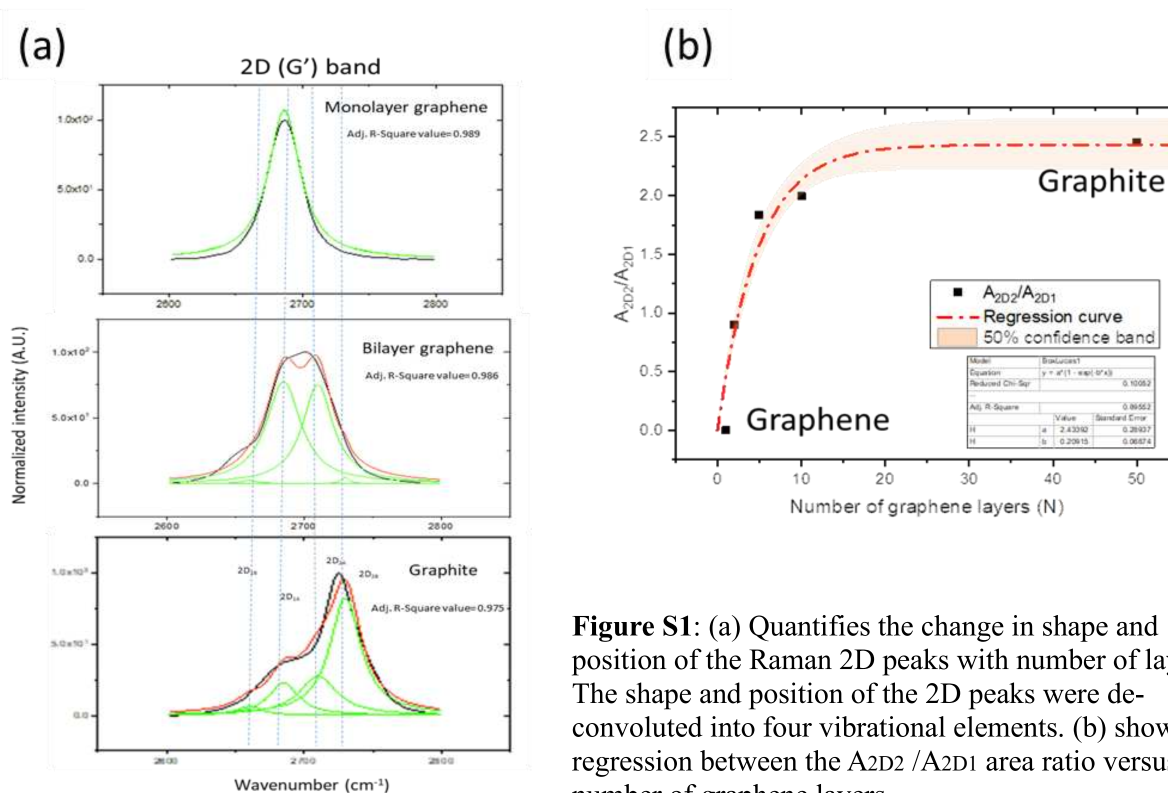

Figure S1: (a) Quantifies the change in shape and position of the Raman 2D peaks with number of layers. The shape and position of the 2D peaks were de-convoluted into four vibrational elements. (b) shows a regression between the A_{2D2} /A_{2D1} area ratio versus number of graphene layers.

evident. This is because the possibility of 2D band scattering processes increase as the number of graphene layer increases. Malard et al. have suggested there are 15 possibilities for a trilayer graphene, but the frequency spacing between each peak is not large enough for them all to be resolved [2]. Although the scattering gets even more complex for multilayer graphene (N>3), the 2D peaks start to merge and become simpler in terms of their overall appearance. For highly oriented pyrolytic graphite (HOPG, $N \rightarrow \infty$), the 2D band can be de-convoluted into two main bands ($2D_{1A}$ and $2D_{2A}$). This was explained as a result of the number of double resonance events allowed in in the three-dimensional structure [3], and has been discussed in detail using a geometrical approach by Cancado et al. [3], [4].

To practically utilise the variation of the 2D peak for experimental study, the ratio of integrated areas: $A_{2D2}/A_{2D1} = (2D_{2A}+2D_{2B}) / (2D_{1B} + 2D_{1A})$ was plotted versus the number of graphene layers. As seen in **Figure S1 (b)**, the A_{2D2}/A_{2D1} ratio increases with the number of graphene layers (N), from 0 for monolayer graphene, to ~ 2.4 for HOPG. An empirical equation was then obtained by fitting the A_{2D2}/A_{2D1} ratio against (N), where the number of graphene layers (N) is then given by:

$$N = \frac{1}{(-0.209 \pm 0.068)} \times ln\left(1 - \frac{A_{2D2}/A_{2D1}}{2.434 \pm 0.289}\right) \dots (equation\ S1)$$

However, in practice, such an equation is difficult to apply for the estimation of the number of graphene layers. This is because the peak fitting process is complex and the relatively weak 2D peak in damaged graphene makes this difficult and time consuming.

S2. Statistically representative sampling for Raman analysis

Random sampling

The population of flakes is much higher than the sampling size we are able to measure. Thus, a random sampling method was implemented to make measurement statistically representative. As mentioned in the experimental section, the graphene suspension was sonicated prior to drop casting onto a 1cm×1cm SiO_2 (285 nm)/Si substrate for microscopic observation. The sonication process is assumed to prevent unwanted sedimentation, so that the suspension is well-mixed. A virtual coordinate was defined on the deposited substrate using the microscope stage. The 1cm×1cm substrate was divided into 10×10 grids, so each grid has a ~1mm×1mm area and can also be located by the stage of the Raman spectrometer. By generating two series

of random numbers between 0 to 10, a random grid was identified for measurement. The Raman measurements were performed on a graphene flake within the randomly identified grid. This is similar to the Monte Carlo method.

Confidence interval

Can these measured flakes represent the quality of the graphene suspension? How confident is the measurement? Statistical interval estimation may shed some light on it. Interval estimation is often used to calculate an interval of possible parameter values of an unknown population based on the observed sample data. The t distribution is a well-accepted method to obtain an unknown population when large scale sampling is unavailable. From the student's t distribution, the population mean (μ) can be estimated using:

$$\bar{x} - t\frac{s}{\sqrt{n}} < \mu < \bar{x} + t\frac{s}{\sqrt{n}}$$

, where n is the sample size, $\bar{x}$ is the mean value of sample and s is sample standard deviation. The value of t is decided by the degree of freedom and the chosen confidence interval and can be found in standard tables for $n < 30$.

Thickness distribution

With 20 randomly selected flakes, we have calculated the sample mean ($\bar{x}$) and standard deviation (s) as 5.6 and 3.4 respectively. With 99% of the confidence interval and $t = 2.9$ (degree of freedom =19), a $3.5 < \mu_{thickness} < 7.8$ (between 4-8 layers) can be determined.

How many flakes should be measured that can effectively represent a solution processed graphene sample? This varies sample by sample, depending on how accurate a measurement is required and how inhomogeneous the flakes are. Assuming we can tolerate an error of 3 layers ($E = 3$), then the confidence interval is 99%. We can estimate $n \geq \left(\frac{ts}{E}\right)^2 = \left(\frac{2.9*3.4}{3}\right)^2 =$ 10.8, meaning we can make a significant measurement if we randomly sample more than 11 flakes from the 2Dtech graphene suspension. The confidence interval can be improved by increasing the number of flakes being sampled. This can be ideal when utilising scanning Raman spectroscopy to avoid human operator bias etc.

Distribution of defect concentration

Similarly, with 20 randomly selected flakes, the 99% confidence interval and a degree of freedom = 19 for the measured flakes gives an estimation that the population mean ($\mu_{I(D)/I(G)}$)

is between $0.12 < \mu_{I(D)/I(G)} < 0.19$. As the measured sample mean $(\bar{x})$ is 0.16, the standard deviation (s) is 0.053 and $t = 2.9$.

S3. The plasmon bands in multilayer graphene / graphite

Surface plasmons can be observed in the low-loss EELS spectra. A noticeable change in both peak shape and position as a function of graphene thickness is apparent and this could be used as an alternative method for characterising the thickness of graphene for flakes that have a

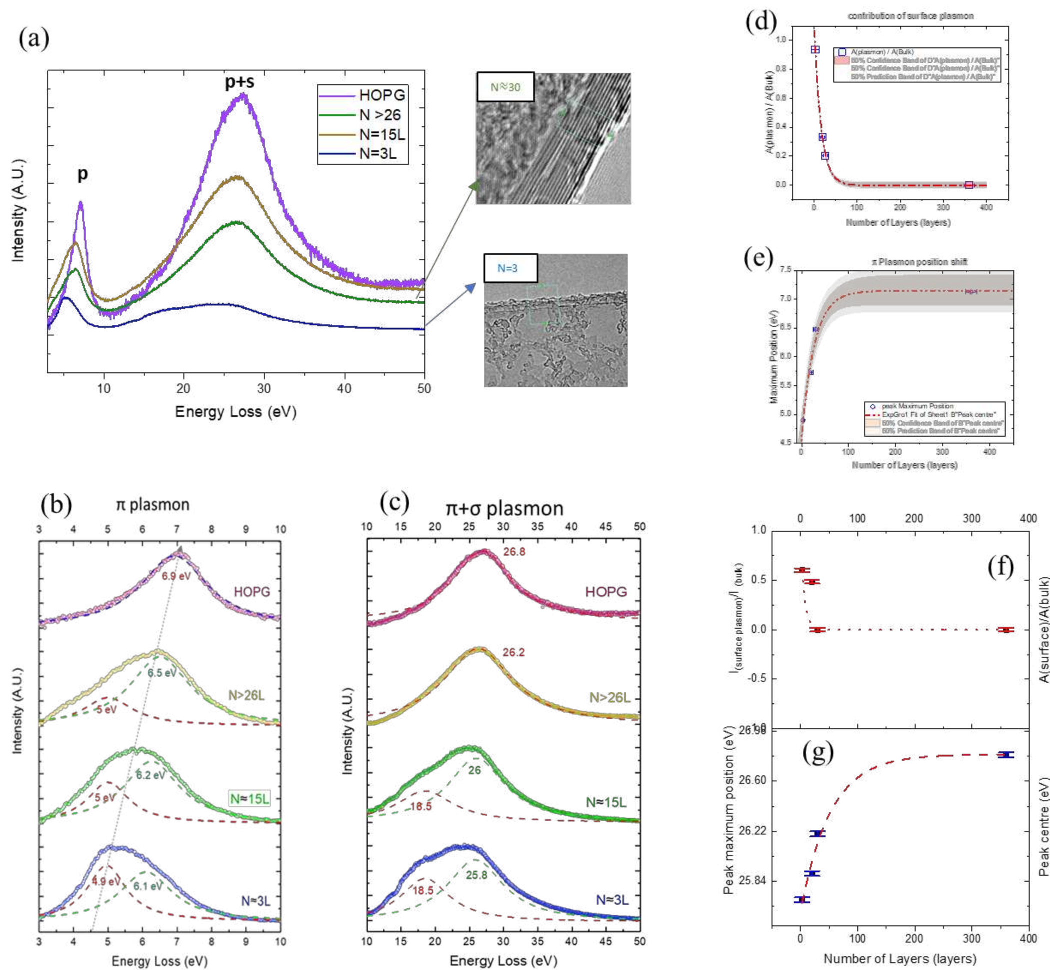

Figure S2: (a) EEL low loss spectra of 3, 15 and 26 layer graphene compared to an HOPG specimen (relative thickness = 1.05). The Zero Loss Peak was approximated by the logarithm tail model and subtracted. The number of graphene layers in a flake was characterised by the folded edge method from TEM images. (b) shows the variation of π plasmon peak with the number of graphene layers, which was fitted with two Lorentzian peaks. (c) shows the variation of the π+σ plasmon peak with the number of graphene layers, which was fitted with two Lorentzian peaks. (d) shows the surface / bulk π plasmon peak intensity ratio as a function of the number of graphene layers. (e) shows the variation of the π plasmon peak position as a function of number of graphene layers. (f) shows the surface / bulk π+σ plasmon peak intensity ratio as a function of the number of graphene layers. (g) shows the variation of the π+σ plasmon peak position as a function of number of graphene layers.

relative thickness (t_R = specimen thickness / inelastic mean free path of electrons) smaller than 0.1. The change in peak position and shape for different graphene thicknesses is shown in **figure S2 (a)** . Here, the ZLP tail was approximated by a logarithmic tail model and the number of graphene layers was determined by counting 002 fringes at their folded edges in the TEM or STEM image. The thickness of an HOPG sample was estimated to be ~360 layers, and a clear π plasmon peak shift towards lower energy loss is accompanied by a $\pi + \sigma$ plasmon peak broadening as the number of graphene layers decreases. The π plasmon peak maximum was found to shifted from ~7 eV in HOPG to ~5 eV in flakes that consisted of 3 layers (**Figure S2 (b)**). This observation agrees with a similar study from Eberlein et al. [5] on free-standing graphene, in which the centre of the π plasmon peak was reported to be 4.7 eV for a free-standing monolayer graphene, and 7 eV for a 30-layer graphite flake. Fitting the plasmon peak with a Lorentzian, as shown in **figure S2(b)**, reveals that the bulk π plasmon peak in HOPG comprises only a Lorentzian peak centered at 6.9 eV. However, as the flakes get thinner, an additional surface plasmon peak at ~5eV becomes observable and of higher relative intensity. **Figure S2(d)** shows the ratio between the integrated areas of the surface and bulk π plasmons which increases from 0 in the HOPG sample to more than 0.9 in a trilayer graphene. The trend can be fitted with an exponential decay function, which confirms that the main contribution to the π plasmon peak is the surface plasmon when the specimen is very thin, while the bulk plasmon π dominates when the specimen is thick.

Due to the differing relative contributions of the surface and bulk plasmons, as seen in **figure S2(e)**, the overall position of the π plasmon peak shifts with the number of graphene layers and, by fitting, the following relationship can be obtained:

$$x_{M\,(\pi)} = (7.15 \pm 0.27) + (-2.55 \pm 0.42)e^{-\frac{N}{(27\pm 9.13)}} \ldots (equation\ S2)$$

, where $x_{M\,(\pi)}$ is the position of the maximum in the π plasmon peak and N is the number of graphene layers. Thus, using equation S1, the number of graphene layers can be estimated from the position of the π plasmon peak as is shown in **figure S2 (e)**.

Similarly in the $\pi + \sigma$ plasmon region, shown in **figure S2(c)**, for thin graphene flakes (<15layers) an additional surface $\pi + \sigma$ plasmon peak centered at 18.5eV is evident in addition to the bulk $\pi + \sigma$ plasmon peak at ~26 eV. The variation in the ratio of relative intensities between the integrated areas of the surface and bulk $\pi + \sigma$ plasmons as a function of the number of graphene layers is shown in **Figure S2(f)**, whilst the corresponding change in overall $\pi + \sigma$ plasmon peak position is shown in **Figure S2(g)**. The overall peak centre progressively

moves towards higher energy with increasing number of graphene layers as the surface plasmon excitation mode vanishes whilst the bulk plasmon mode remains. Comparing the results from **figure S2** to the conventional log-ratio method for thickness determination, discussed in section 3.1, the variation of plasmon peak position shows a more sensitive trend versus graphene flake thickness, particularly for very thin flakes. Further details of plasmons in graphene can be found in reference [5].

S4. The resolution of the optical microscope

Traditionally, the lateral resolution limit can be calculated via Abbe's formulation [6]: $Min[\Delta r_{\|}] = 0.61\frac{\lambda}{NA}$, where $Min[\Delta r_{\|}]$ is the minimum distance that can be resolved in the object plane, λ is the wavelength of light and NA is the numerical aperture of the objective lens. Within the visible light range (380-750 nm), a $Min[\Delta r_{\|}] \approx 0.26\,\mu m$ was estimated in our system (NA=0.95) and thus graphene features smaller than this $Min[\Delta r_{\|}]$ cannot be resolved. Nevertheless, Abbe's formulation is based on a variety of assumptions to simplify the calculation and the resolution may actually exceed the limits when using modern digitalised optical microscopy. However, the true resolution of the optical microscope can be determined by a Fourier-based method. The two-dimensional Fourier transform (or power spectrum) of an image can be obtained by applying fast Fourier transform (FFT) algorithms [7], [8], in which the intensity of the frequency spectrum of the content in a micrograph is plotted as a function of the spatial frequency with the zero frequency being at the centre of the transform. **Figure**

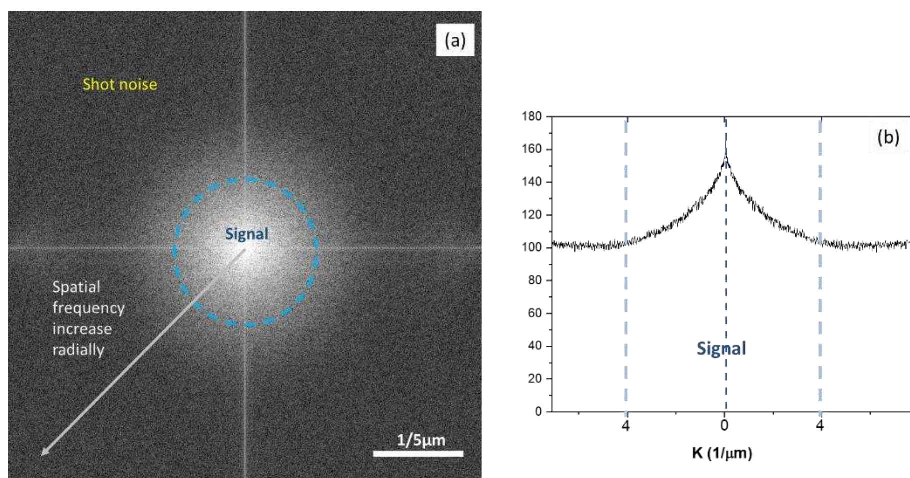

Figure S3: (a) the power spectrum of the micrograph in **Figure 9;** (b) shows the radial intensity profile of **figure S1(a)** where the signal boundary is 4.0±0.5 (1/μm), corresponding to a resolution limit of 0.25±0.03 μm.

S3 **(a)** shows the power spectrum of the micrograph of **Figure 9 (a)**. The signal intensity (represented here by the brightness of the image) decreases with increasing frequency until it eventually vanishes into the random noise background of the microscope image. The spatial frequency at which the SNR falls below the minimum value required to satisfy the Rose criterion is the limit to the information that can be resolved [7], [8]. **Figure S3 (b)** shows the intensity profile across **Figure S3 (a)** and, as both Joy and Lorusso et al have suggested, the value of signal boundary is where the intensity vanishes below the background noise [7], [8]. In the case of **Figure S3,** the signal boundary is 4.0±0.5 (1/µm), and the resolution limit of our optical microscope setup is 0.25±0.03 µm, which agrees with Abbe's formulation.

S5. The precision of lateral flake size measurement using OM

To understand the precision of flake selection and lateral size measurement using the optical image filtering method, the original OM image can be compared to an overlayed filtered image of selected graphene flakes. As shown in **figure S4 (a)**, the original OM image consists of background and both thick and thin flakes**. Figure S4 (b)** shows flakes that were selected using the image filtering method; thin flakes appear blue and were selected for analysis, with thick flakes excluded. **Figure S4 (c)** compares the pixel intensity profiles in the green channel across the same flake as indicated by the black and red arrows in **Figure S4 (a) and (b)**, respectively.

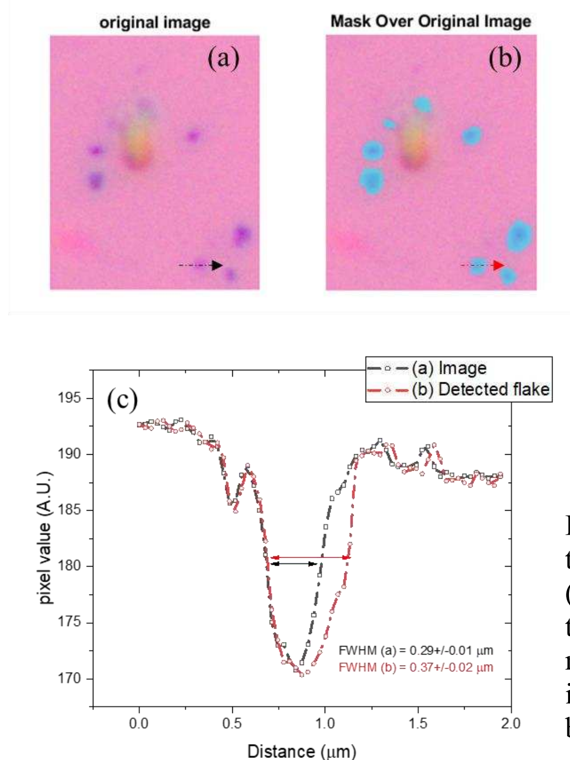

Figure S4: Compares an original OM image (a) to the corresponding image of selected flakes (b). The blue patches in figure (b) show flakes that were selected using the image filtering method. (c) compares the pixel intensity profile in the green channel across the flake identified by the arrows in figures (a) and (b).

The profile from the original image shows a FWHM of 0.29±0.01μm, while following filtering and flake selection, the profile shows a FWHM of 0.37± 0.02 μm, which is about 27% bigger than in the original image. Due to the limited spatial and colour resolution, a different thresholding value could result in a deviation in the measured lateral dimension. However, in practice, little difference in the distribution of lateral dimensions is observed when it is obtained from a large area (i.e. number of flakes), presumably because the uncertainty in flake dimension due to lack of spatial resolution is compensated for by a larger sampling size.

Reference

[1] A. C. Ferrari *et al.*, "Raman Spectrum of Graphene and Graphene Layers," *Phys. Rev. Lett.*, vol. 97, no. 18, p. 187401, Oct. 2006.

[2] L. M. Malard, M. H. D. Guimarães, D. L. Mafra, M. S. C. Mazzoni, and A. Jorio, "Group-theory analysis of electrons and phonons in N -layer graphene systems," *Phys. Rev. B - Condens. Matter Mater. Phys.*, vol. 79, no. 12, Dec. 2009.

[3] K. F. Mak, M. Y. Sfeir, J. A. Misewich, and T. F. Heinza, "The evolution of electronic structure in few-layer graphene revealed by optical spectroscopy," *Proc. Natl. Acad. Sci. U. S. A.*, vol. 107, no. 34, pp. 14999–15004, 2010.

[4] L. G. Cançado, A. Reina, J. Kong, and M. S. Dresselhaus, "Geometrical approach for the study of G′ band in the Raman spectrum of monolayer graphene, bilayer graphene, and bulk graphite," *Phys. Rev. B - Condens. Matter Mater. Phys.*, vol. 77, no. 24, p. 245408, Jun. 2008.

[5] T. Eberlein *et al.*, "Plasmon spectroscopy of free-standing graphene films," *Phys. Rev. B - Condens. Matter Mater. Phys.*, vol. 77, no. 23, p. 233406, Jun. 2008.

[6] L. L. Novotny, *Principles of Nano-Optics*, 2nd ed., vol. 1, no. 4. Cambridge University Press, 2006.

[7] D. C. Joy, "SMART - A program to measure SEM resolution and imaging performance," *J. Microsc.*, vol. 208, no. 1, pp. 24–34, 2002.

[8] G. F. Lorusso and D. C. Joy, "Experimental resolution measurement in critical dimension scanning electron microscope metrology," *Scanning*, vol. 25, no. 4, pp. 175–180, 2003.